Evaluating the fidelity and robustness of calibrated numerical model predictions

An application on a wind turbine blade

Garrison Stevens
Glenn Department of Civil Engineering, Clemson University, Clemson, South Carolina, USA
Kendra Van Buren
Engineering Institute, Los Alamos National Laboratory, Los Alamos, New Mexico, USA, and
Elizabeth Wheeler and Sez Atamturktur
Glenn Department of Civil Engineering, Clemson University, Clemson, South Carolina, USA

Received 3 September 2013
Revised 6 August 2014
Accepted 27 August 2014

Abstract

Purpose – Numerical models are being increasingly relied upon to evaluate wind turbine performance by simulating phenomena that are infeasible to measure experimentally. These numerical models, however, require a large number of input parameters that often need to be calibrated against available experiments. Owing to the unavoidable scarcity of experiments and inherent uncertainties in measurements, this calibration process may yield non-unique solutions, i.e. multiple sets of parameters may reproduce the available experiments with similar fidelity. The purpose of this paper is to study the trade-off between fidelity to measurements and the robustness of this fidelity to uncertainty in calibrated input parameters.

Design/methodology/approach – Here, fidelity is defined as the ability of the model to reproduce measurements and robustness is defined as the allowable variation in the input parameters with which the model maintains a predefined level of threshold fidelity. These two vital attributes of model predictiveness are evaluated in the development of a simplified finite element beam model of the CX-100 wind turbine blade.

Findings – Findings of this study show that calibrating the input parameters of a numerical model with the sole objective of improving fidelity to available measurements degrades the robustness of model predictions at both tested and untested settings. A more optimal model may be obtained by calibration methods considering both fidelity and robustness. Multi-criteria Decision Making further confirms the conclusion that the optimal model performance is achieved by maintaining a balance between fidelity and robustness during calibration.

Originality/value – Current methods for model calibration focus solely on fidelity while the authors focus on the trade-off between fidelity and robustness.

Keywords Uncertainty quantification, Validation, Experimental modal analysis, Prediction accuracy, Self-consistency, Test-analysis correlation

Paper type Research paper

The authors thank Francois Hemez of Los Alamos National Laboratory and Yakov Ben-Haim of Technion Israel Institute of Technology for the assistance with info-gap decision theory. The authors also wish to express the gratitude to Stuart Taylor of Los Alamos National Laboratory for supplying the experimental configuration and modal analysis measurements of the CX-100 wind turbine blade, and to D.J. Luscher for supplying the scripts for the NLBeam geometrically exact beam model.

Engineering Computations: International Journal for Computer-Aided Engineering and Software
Vol. 32 No. 3, 2015
pp. 621-642

0264-4401
DOI 10.1108/EC-09-2013-0217

Nomenclature

α	horizon of uncertainty	$\tilde{u}$	uncertain input parameters at nominal setting
$\hat{\alpha}$	robustness	Y_e	experimental observations
$M(u)$	simulation model	Y	simulation predictions
R_C	critical performance level		
U	info-gap uncertainty model		
U	uncertain input parameters		

1. Introduction

Wind energy is being pursued as a viable source of energy in the USA due to its forecasted potential to supply 20 percent of the nation's energy needs by 2030 (US Department of Energy, 2008). To meet these expectations, wind turbine production in the USA has expanded from rotors with a diameter of 18 meters in 1985 to 120 meters in 2007 (Ashwill, 2009). To better understand the performance of wind turbines produced at this massive scale, modeling, and simulation techniques are being implemented at an increasing rate. In recent studies, numerical models have been demonstrated to be useful tools to study the performance of individual wind turbine blades, such as the tip deflection (Bechly and Clausen, 1997), failure (Shokrieh and Rafiee, 2006; Marin *et al.*, 2009), and interaction with wind loading (Brazilevs *et al.*, 2011). Furthermore, plant scale simulations have been demonstrated to be useful in planning the expansion of wind turbine plants (Sprague *et al.*, 2011), optimizing power output (Sanderse *et al.*, 2011), and minimizing fatigue failure (Vermeer *et al.*, 2003).

Although numerical modeling has been gaining increased acceptance in wind engineering, the limitations to analyze the performance of engineering systems in a predictive capacity must be emphasized. Only through rigorous evaluation of inherent uncertainties and errors in model predictions through systematic comparisons against measurements can numerical models be used in a predictive capacity. Figure 1 depicts the prevailing engineering approach to predictive modeling, where a model is used to predict the response of configuration[1] "A," which is infeasible to experimentally measure (such as in-service performance of wind turbines). Here, experimental measurements (such as experimental modal data) are only available for response at configuration "B," which can be used to calibrate the model. This calibrated model[2], which is conditioned upon the available experiments, is then used to predict untested configurations, i.e. configuration "A" (McFarland and Mahadevan, 2008; Unal *et al.*, 2011; Hegenderfer and Atamturktur, 2013). As seen, the success of predictive modeling relies on the success of model calibration (Atamturktur *et al.*, 2012). This is especially important for numerical models of wind turbine blades, where experimental modal analysis has been heavily pursued to provide evidence for calibration of models that

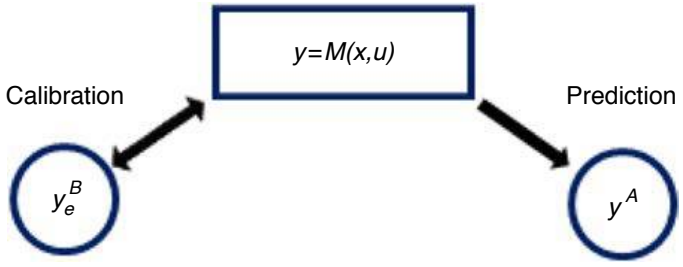

Figure 1.
FE model calibration and prediction process

are used to predict for instance, in-service performance (Griffith *et al.*, 2008; Van Buren and Atamturktur, 2012).

There are two fundamental premises behind the process shown in Figure 1. First, y_e^B is mechanistically related to y^A in that they share basic physics principles. Second, the calibrated input parameter values are representations of "realistic" parameter values and can be used in making predictions. In this paper, we focus on the latter premise, which is regularly violated during parameter calibration due to the inevitable compensations between various forms of errors and uncertainties inherent in a model.

There are often multiple parameter sets which can reproduce measurements with similar fidelity owing to for instance the insufficient quality and quantity of experiments, unavoidable imperfectness of our numerical models, collinearity between model parameters and, etc. Among these multiple solutions, there may be one parameter set that yields best fidelity. However, given the unknown compensations between various forms of uncertainties and errors, the meaning of the best fidelity model becomes questionable making the selection of this particular set hard to justify. This of course reduces our confidence in the calibrated parameter values.

The problem is further complicated when one considers the systematic biases in model predictions which originate from both the intentional simplifications made during the model development and unforeseen omissions of physics phenomena from the model due to lack of knowledge (Draper, 1995; Goulet and Smith, 2013). The presence of model bias can be addressed by calibrating the model parameters and simultaneously training an independent error model as suggested by Kennedy and O'Hagan (2001) and implemented in Higdon *et al.* (2008). Neglecting the presence of model bias in model calibration is shown to yield parameter values that compensate for the bias (Atamturktur *et al.*, 2014). However, proper determination of bias depends heavily on the availability of a sufficient number of informative experiments throughout the operational domain of interest and one must be careful that for experiment-poor situations as inaccurate training of bias model may further degrade the predictions (Atamturktur *et al.*, 2011, 2014). Regardless of whether bias is explicitly considered in model calibration or not, the central question that remains is whether these models with calibrated input parameter values can be used in a predictive capacity.

Recent studies have proposed calibration methods to develop models that exhibit robustness by considering the trade-offs between the fidelity of model predictions to measurements and robustness of this fidelity to uncertainty in model parameters (Hemez and Ben-Haim, 2004; Pereiro *et al.*, 2013; Atamturktur *et al.*, 2014). Calibrated models that exhibit *robustness* continue to yield solutions with sufficient fidelity to measurements when uncertainties resulting from our lack of confidence in calibrated parameter values are accounted for. Note that in this approach both fidelity to measurements and robustness of this fidelity to uncertainties are evaluated at the tested configurations (i.e. configuration "B" in Figure 1). The development of credible numerical models must also consider the credibility of the model predictions at untested configurations (i.e. configuration "A" in Figure 1), herein referred to as self-consistency of predictions. Self-consistency, only recently being recognized (Ben-Haim and Hemez, 2012), is defined herein as the consistency (i.e. lack of variability) in model predictions at untested configurations when lack of confidence in the calibrated input parameter values is accounted for. Due to the

difficulty in developing reliable probability models to express such lack of confidence in calibrated parameter values, non-probabilistic methods are preferable to study the concept of robustness. Info-gap decision theory, discussed in more detail in Section 2 of this manuscript, supplies one such non-probabilistic method to quantify the robustness of model predictions against uncertainty in calibrated input parameter values.

In this paper, the authors demonstrate the aforementioned concepts on the development of a calibrated one-dimensional (1D) finite element (FE) model of a wind turbine blade. The selection of this case study is motivated by the need for simplified, yet sufficiently accurate, wind-turbine blade models that can be incorporated into large-scale simulations and coupled with fluid dynamic models simulating airflow (Linn and Koo, 2011). Such simplified FE models maintain low computational cost and thus, are exceedingly useful for applications such as plant scale simulations (Fleming and Luscher, 2014). Figure 2 illustrates the steps followed in the development of the calibrated 1D FE model for the CX-100 wind turbine blade, developed at Sandia National Laboratory. Section 3 summarizes the steps taken to derive equivalent 1D parameters from a three-dimensional (3D) FE model of the CX-100 blade. Sections 4 and 5 present the experimental campaign and calibration of the linear 1-D model against this experimental data, respectively. In Section 6, the linear 1-D model is extended into the nonlinear range by considering geometric nonlinearities and the self-consistency of calibrated model predictions are evaluated at an untested loading scenario, namely in predicting deflection. In Section 7, the weighted sum method (WSM) for Multi-criteria Decision Making (MCDM) is applied to determine the calibration solution from Section 6 that best meets the fidelity, robustness, and self-consistency criteria simultaneously.

2. Overview of info-gap decision theory

Info-gap decision theory provides a non-probabilistic approach that can be used to quantify the effects of uncertainty in the input parameters on the output response of a system. In the info-gap approach, the uncertain input parameters are described using

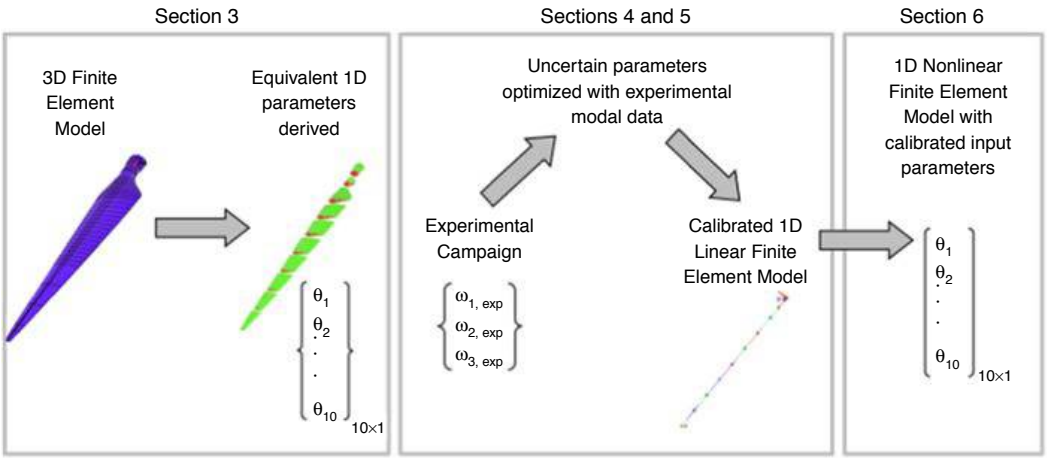

Figure 2.
Flowchart for Identification of model parameters

monotonically increasing, unbounded convex sets. The need to assume a particular probability distribution is eliminated by accepting the uncertain input parameters to assume values that are clustered, a premise which can be justified for many engineering parameters.

Let us assume a numerical model, M, representing the relationship between the input parameters, u, and output, y:

$$y = M(u) \tag{1}$$

Herein, the uncertainty of concern is due to the non-unique sets of model parameters that yield model predictions with similar fidelity to experiments. This uncertainty originates during the model calibration process as a result of the unknown compensations between various forms of uncertainties and errors owing to for instance the unavoidable scarcity of calibration experiments, inherent uncertainty in measurements, inevitable incompleteness of our numerical models, collinearity of model parameters and, etc.

For configurations in which experimental data is available (recall configuration B in Figure 1), fidelity of a model can be defined as the difference between the model predictions, y and measurements, y_e calculated using a user-defined norm. Herein, the performance $R(u)$ will be considered acceptable when an established critical performance level, R_C, is fulfilled (as seen in Figure 3), i.e. $R(u) \leqslant R_C$:

$$R(u) = \|y - y_e\| \tag{2}$$

On the other hand, for configurations in which experimental data is unavailable (recall configuration A in Figure 1), the performance of the model can be defined by the self-consistency of predictions, y with respect to the predictions of the model obtained with nominal parameter values, y_n calculated once again using a user-defined norm. Here, nominal parameter values refer to the best estimate values determined through calibration of the model against available experiments:

$$R(u) = \|y - y_n\| \tag{3}$$

The info-gap uncertainty model, U, then describes how the performance of the system varies around the nominal model (i.e. the model with nominal parameter values) for a given horizon of uncertainty, α. When $\alpha = 0$, the uncertain input parameters remain at their nominal setting, $\tilde{u}$ (i.e. our best estimate). When $\alpha \neq 0$, the input parameters are allowed to vary within a convex set represented by U. The objective is then to find the model with worst case performance within this convex set of input parameters. In an envelope-bound info-gap uncertainty model, the uncertainty space is defined using a percentage difference between the nominal parameter values, $\tilde{u}$ and the uncertain parameter values, u (Ben-Haim, 2006):

$$U(\alpha; \tilde{u}) = \left\{ u : \left| \frac{u - \tilde{u}}{\tilde{u}} \right| \leqslant \alpha \right\}, \quad \alpha \geqslant 0 \tag{4}$$

As α increases, the convex set gets bigger and thus, finding new parameter sets with worst case performance becomes possible. The worst case performance is then evaluated at each level of horizon of uncertainty, α. The robustness, $\hat{\alpha}$ is defined as the

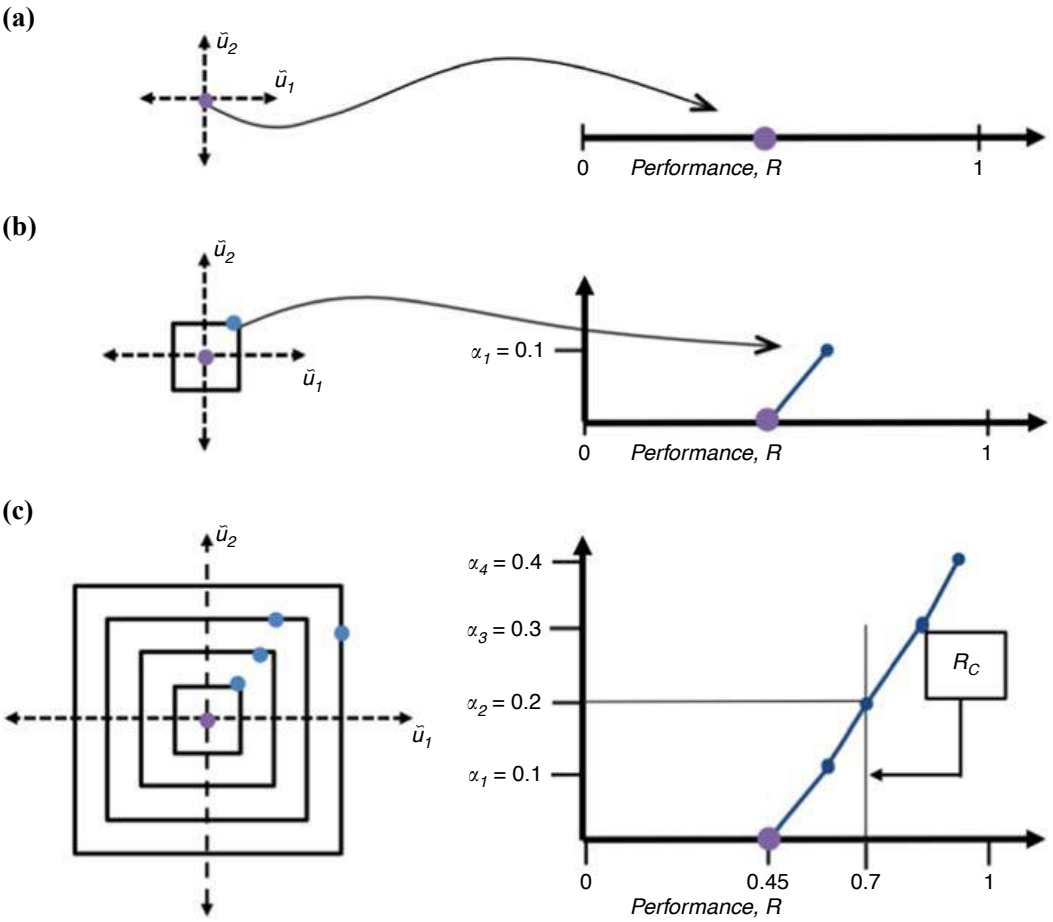

Figure 3.
Illustration of a hypothetical info-gap robustness

Notes: (a) Performance at $\alpha = 0$; (b) development of robustness curve; (c) info-gap robustness

maximum horizon of uncertainty at which the worst case performance still satisfies the critical performance level, R_C, as represented in Equation (5).

$$\hat{\alpha} = \max\left\{\alpha : \left(\max_{u \in U(\alpha;\tilde{u})} R(u)\right) \leqslant R_C\right\}, \quad \alpha \geqslant 0 \tag{5}$$

Note that the critical performance level, R_C need not be determined beforehand in Equation (5) so that the model performance can be evaluated for a range of critical performance levels to aid in the decision-making process (Hemez and Ben-Haim, 2004). This can be accomplished by the development of robustness curves, demonstrated in Figure 3 for a hypothetical model with two uncertain parameters, u_1 and u_2. Figure 3 (a) shows the evaluation of the nominal performance at the nominal parameter values (i.e. α is set to 0). However, if α is set to 0.1, it becomes possible to find a (u_1, u_2) pair that results in performance less than the nominal performance. Repeating the process with increasing horizons of uncertainty, α results in the development of a robustness curve, demonstrated in Figure 3(b). From a practical standpoint, development of robustness curves requires an analysis wherein the uncertainty space is searched to determine the parameter set that yields the worst performance, R for each horizon of uncertainty.

Figure 3(c) is the resulting info-gap robustness curve for four levels of the horizon of uncertainty evaluated in increments of 10 percent uncertainty in the parameters (i.e. $\alpha_1 = 0.1$, $\alpha_2 = 0.2$, $\alpha_3 = 0.3$, and $\alpha_4 = 0.4$). According to the robustness curves shown in Figure 3(c), to obtain a performance of $R_C = 0.45$ from the system in Figure 4, parameters u_1 and u_2 must be known with zero uncertainty. However, suppose the critical performance requirement, R_C is set to 0.7 then, 20 percent uncertainty in the input parameters can be tolerated. As seen, only by relaxing the fidelity requirement will the range of permissible variation in the parameters and thus, robustness increase.

A robustness curve with a large slope, "$\Delta\alpha/\Delta R$," as shown in Figure 4(a), indicates that the model predictions are less sensitive to increasing levels of uncertainty, α whereas a robustness curve with a small slope, as shown in Figure 4(b), indicates the model predictions are more sensitive to uncertainty in parameters. Clearly, a large robustness is more desirable as it means the model is capable of accommodating greater uncertainties in model parameters without significantly sacrificing performance (i.e. fidelity). When the performance of the model can be no worse than $R_C = 0.6$, the amount that the parameters are allowed to vary in Figure 4(a) corresponds to a horizon of uncertainty of $\hat{\alpha} = 0.2$. On the contrary, Figure 4(b) demonstrates small robustness, in that the predictions of the model are sensitive to the values of u and little uncertainty can be tolerated without compromising performance. Here, when the performance is $R_C = 0.6$, the allowable uncertainty is only $\hat{\alpha} = 0.05$. As seen, robustness curves supply a powerful comparative tool that can be used for evaluating the robustness of a family of calibrated models.

3. Development of simplified 1D Model: CX-100 blade

In Van Buren *et al.* (2012), a 3D FE model of the CX-100 turbine blade was built in ANSYS v. 12 using the geometry of the blade provided in the design specifications. The numerical uncertainties in this 3D model were evaluated through an in depth verification study in Mollineaux *et al.* (2012). The 3D model was then calibrated against natural frequencies measured during the tests conducted at Los Alamos National Laboratory (Farinholt *et al.*, 2012), and validated against mode shapes using modal assurance criterion (Van Buren *et al.*, 2012). Herein, this 3D model is employed to approximate the initial values of the properties for the 1D beam model.

The 3D model of the wind turbine blade is discretized into equivalent 1-meter sections with an additional node placed at the 0.675 meter station to capture the effects of the tapering root section (Figure 5). A more refined discretization, i.e. smaller size

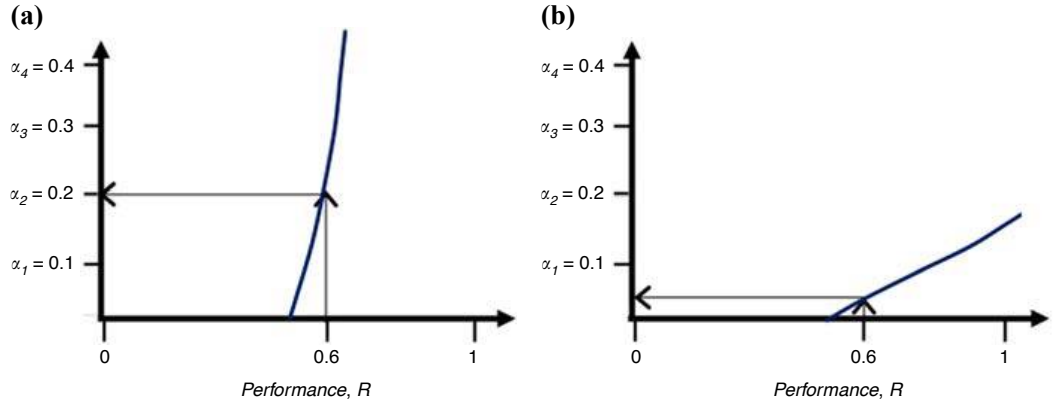

Notes: (a) Large robustness; (b) small robustness

Figure 4. Conceptual representation of robustness

sections, is deemed unnecessary as the modal parameters of the 1D beam model are observed to converge with nine elements. These nine sections are analyzed individually to provide equivalent model parameters for each of the nine elements of the 1D model that is built using Beam189 elements in ANSYS v. 12. The mass contribution of each section is identified, providing an estimate for the equivalent density for individual sections of the 1-D model. The cross-sectional area, effective Young's modulus, and area moments of inertia are approximated for each section by averaging the values measured at the beginning and end of the section. The cross-sectional area is calculated by multiplying the total cross-sectional element lengths by the material thickness of each element within a section. The Young's modulus is calculated using an area proportional weighting. Lastly, the area moments of inertia are derived by individually calculating and summing the area moment of inertias for all elements in the cross-section. Table I lists the initial estimates for the equivalent beam properties.

In this list, the equivalent area moment of inertia and the Young's modulus are the most challenging parameters to define accurately. Note that these two parameters exercise similar effects on the stiffness distribution of the blade, and thus, herein only the moment of inertia values of each of the ten sections are selected for calibration. Similarly, the study could have been completed solely focussing on the calibration of the Young's modulus values.

4. Experimental campaign and model calibration

4.1 Experimental campaign and test analysis correlation

An experimental modal analysis campaign is completed on the CX-100 wind turbine blade at the National Renewable Energy Laboratory (Farinholt *et al.*, 2012) under the

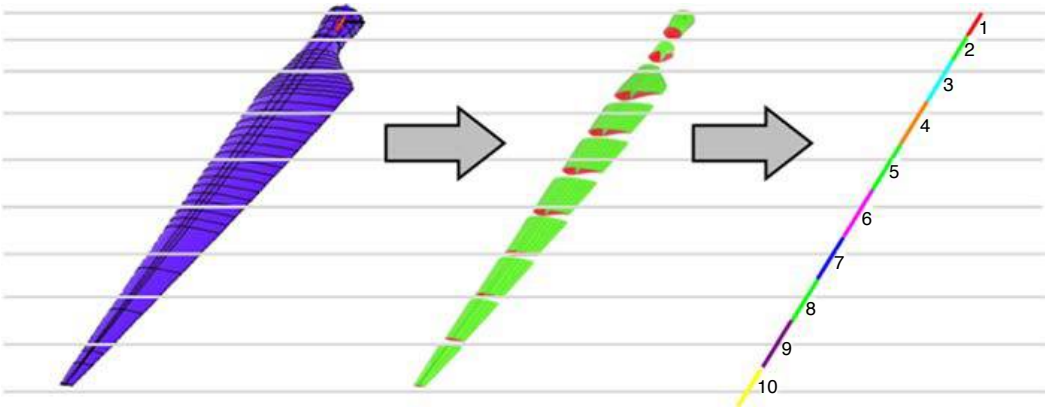

Figure 5.
Deriving equivalent beam model properties of the CX-100

Section	Area (m^2)	Mass (kg)	Density (kg/m^3)	I_{xx} (m^4)	I_{yy} (m^4)	I_{xy} (m^4)	E (GPa)
1	0.0321	55.99	2,584.1	0.00052	0.00051	3.22E-06	36.01
2	0.0133	8.35	1,929.3	0.00020	0.00015	3.40E-05	24.33
3	0.0177	19.45	1,097.2	0.00111	0.00023	0.00030	22.19
4	0.0199	18.88	949.0	0.00161	0.00022	0.00040	13.34
5	0.0169	16.37	967.5	0.00104	0.00010	0.00019	6.29
6	0.0129	12.69	981.0	0.00061	4.58E-05	8.11E-05	8.19
7	0.0093	7.36	794.8	0.00031	1.66E-05	3.00E-05	10.04
8	0.0073	5.38	736.5	0.00014	6.01E-06	8.89E-06	10.51
9	0.0051	3.75	739.2	5.05E-05	1.76E-06	1.52E-06	10.07
10	0.0028	2.08	754.1	1.31E-05	3.73E-07	4.00E-07	8.61

Table I.
Initial estimates of the equivalent beam properties

fixed free conditions with the blade mounted to a seven-ton steel frame. Modal testing is performed using a roving impact hammer test with four uni-axial accelerometers and one tri-axial accelerometer. Response measurements are obtained for 65 impact locations: 47 in the flapwise direction, and 18 in the edgewise direction. Three test repeats are performed with a linear average and 150 Hz sampling frequency. The acceleration response is collected with 4,096 sampling points in 11 seconds (Figure 6).

Table II provides a comparison of the first three flapwise experimentally measured frequencies and the 1D FE model defined with the properties listed in Table I. For the purposes of this study, the prediction error, which is as high as 40.9 percent, is deemed unacceptable for the intended use of the model. To improve the agreement between model predictions and experiments, the model will be calibrated against experiments.

4.2 Model calibration with genetic algorithm

In this proof-of-concept application, the area moment of inertia values of the 1D model, listed earlier in Table I, are deemed to be suitable candidates for model calibration. A correction factor, applied as a multiplier, is defined for the area moment of inertia for each section, thus requiring ten correction factors to be calibrated using the experimental measurements. The correction factors are allowed to vary between 0.7 and 1.5, where a value of 1.0 indicates no change in their values.

To reduce computation demands, the 1D FE model is replaced with an emulator in the calculation of the natural frequencies. A cubic polynomial emulator is trained using a hybrid of full factorial and central composite design of experiments of the ten uncertain

Figure 6.
Experimental set-up (left) and base fixity (right)

Mode	Experimental frequency (Hz)	Simulated frequency (Hz)	% Difference
1st flapwise bending	4.35	3.90	−10.3
2nd flapwise bending	11.51	9.78	−15.0
3rd flapwise bending	20.54	12.13	−40.9

Table II.
Comparison of frequencies

correction factors. A mode-by-mode error quantification of the natural frequencies of the 1D model and the 3D model is shown in Table III. Additionally, Figure 7 demonstrates the goodness-of-fit of the polynomial emulator adapted for this study.

Herein, calibration of correction factors is completed through genetic algorithm optimization. Genetic algorithm is a stochastic optimization tool, rooted in providing randomness by mimicking biological behaviors and implementing the survival of the fittest principle (Mitchell, 1998). The algorithm randomly generates an initial population from a user defined range of plausible values with a user-defined number of individuals, which in our case is set to 20. The objective function, which herein is the root mean square difference of the first three flapwise frequencies, is utilized to score and rank each parameter set (Equation (7)):

$$R = \sqrt{\sum_{i=1}^{3} \left(\omega_{sim,i} - \omega_{\exp,i}\right)^2}. \tag{7}$$

After ranking of parameter sets, a new population is formulated using elite individuals, mutations, and crossovers. The elite individuals of the population are simply those with the highest rank. The remaining individuals are used as parents to develop mutations and crossovers. Mutations occur when parameters are randomly changed, and crossovers are developed by randomly combining parameter sets. The algorithm then iterates over a number of generations, which in our study is set to 100.

Table III. Goodness-of-fit of the polynomial emulator

Mode	1D model frequency (Hz)	Emulator frequency (Hz)	% Difference
1st flapwise bending	3.90	3.67	6.1
2nd flapwise bending	9.78	9.77	0.1
3rd flapwise bending	12.13	17.28	−35.0

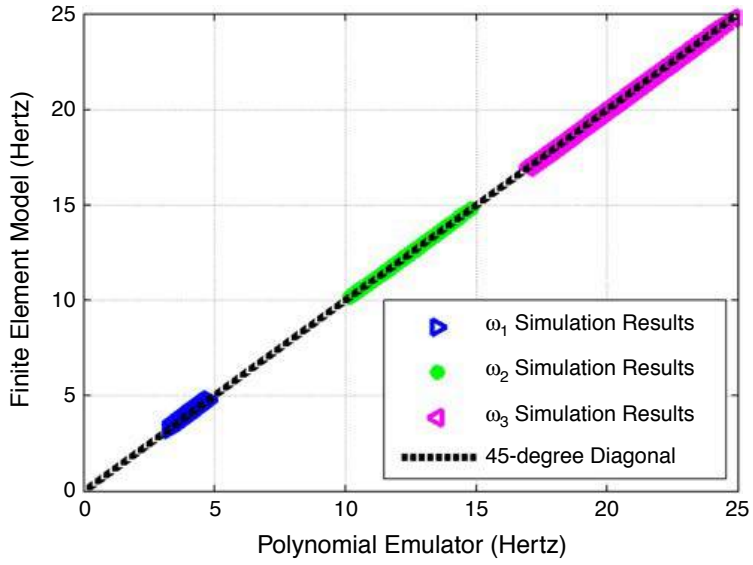

Figure 7. Goodness-of-fit of the polynomial emulator

Calibration considering fidelity only. Defining the objective function of the genetic algorithm using the relationship provided in Equation (7) creates a fidelity optimal model. A fidelity optimal model would be able to reproduce experimental data with great fidelity to measurements, which, however, would only be guaranteed when uncertainties remaining in the calibrated parameter values are neglected. To investigate the trade-off between the fidelity of the model to measurements and the robustness of this fidelity to uncertainty, info-gap decision theory is implemented using an envelope-bound uncertainty model (recall Equation (4)).

Figure 8 compares the robustness of the model developed with the initial parameter estimates given in Table I and the fidelity-optimal model developed with the parameters optimized by genetic algorithm, i.e., before and after calibration of the correction factors. Several observations can be garnered from Figure 8. First, the calibrated, fidelity optimal model is capable of achieving a performance of $R = 0$, however, the model possesses zero robustness in order to achieve this performance. As the critical performance criterion, R_C is relaxed, higher variability is allowed in the model parameters. For example, if the performance requirement of the model is reduced to 0.2 Hz, then the allowable horizon of uncertainty increases to 0.03, as indicated by the dashed lines in the figure. Also illustrated in Figure 8 is the preference reversal indicating that for a performance requirement, R_C less than 0.77 Hz, the fidelity optimal, "calibrated" model is preferable as it yields more robust solutions; however, for R_C greater than 0.77 Hz, the initial, "uncalibrated" model becomes preferable.

In Figure 8, note that the slope of the robustness curve, "$\Delta\alpha/\Delta R$," is less for the calibrated model compared to the uncalibrated model. This indicates that the wind turbine blade model is less robust to uncertainty after calibration than it was before calibration. This is an extremely important point to note, as it brings to attention a critical flaw that has been made too frequently in existing literature. Calibrating parameters of a model with the sole objective of improving agreement between model predictions and measurements leads to a degradation in the robustness of these models. Robustness is an important factor to consider during model calibration

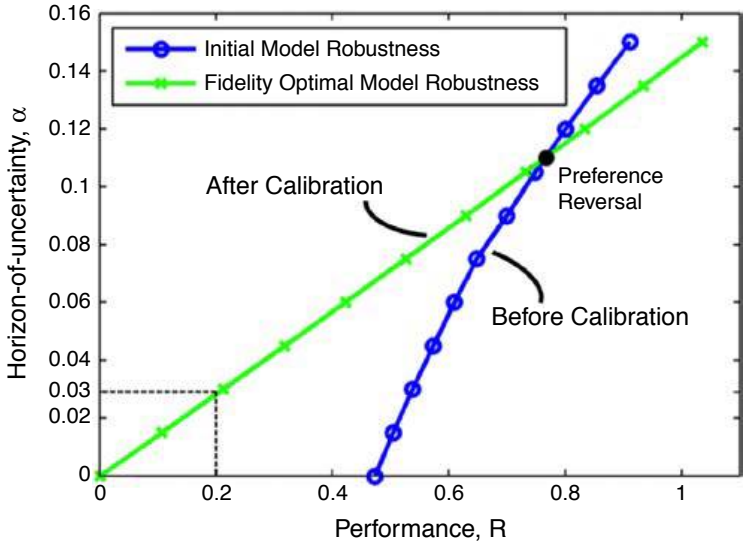

Figure 8.
Info-gap robustness of fidelity-optimal model compared to nominal model

to confirm that unknown compensations between parameters are of low significance on the predictions of calibrated models. Therefore, considering a trade-off between fidelity to data and robustness to uncertainty must be an integral component of model calibration process.

Calibration considering both fidelity and robustness. To include the robustness to uncertainty in the model calibration process, the objective function previously provided in Equation (7) is modified as follows:

$$objective = (w_1 \times R) + (w_2 \times A_r) \tag{8}$$

where R reflects the fidelity of the model defined by the error between predictions and experiments and A_r is the robustness indicator defined by the area above the robustness curve. Here, reduced R indicates increased fidelity and reduced A_r indicates increased robustness. Thus, the optimization problem involves minimizing the objective function given in Equation (8). Weighting functions, w_1 and w_2 are used to control the relative importance of the two competing objectives, where the sum of w_1 and w_2 is one[3].

The robustness indicator used in the objective function, A_r is demonstrated in Figure 9. In the calculation of A_r, the maximum uncertainty in the correction factors is assumed to be known (i.e. 0.1); however, the same area computation can easily be completed for a known R_C. It is important to emphasize that the quantification of robustness as the area, A_r captures the characteristics of the robustness curve, where a smaller area describes a system with larger robustness (Figure 9(a)), and a larger area describes a system with smaller robustness (Figure 9(b)).

During genetic algorithm optimization, the robustness curves are generated for each individual in the population according to which the area above the robustness curve, A_r is calculated. This treatment requires a nested optimization: the outer genetic algorithm optimization searches for candidate solution based on the objective function given in Equation (8), while the inner optimization performs the info-gap analysis and calculates the area above the robustness curve for each individual in the population and of course fidelity to measurements, for each generation.

Of course, the genetic algorithm solutions are sensitive to the weighting factors adapted in Equation (8) (Richardson *et al.*, 1989; Caramia and Dell´Olmo, 2008;

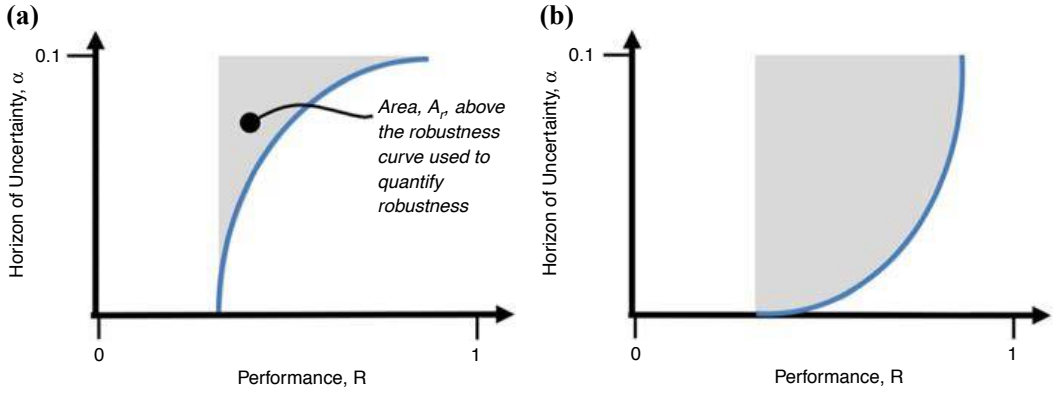

Figure 9.
Quantification of robustness indicator for the objective function

Notes: (a) Large robustness indicator; (b) small robustness indicator

Goel and Stander, 2007), meaning that each pair of weighing factors would yield a different compromise between fidelity and robustness. Hence, we consider five different combinations of weighting factors. A fidelity optimal model is obtained by applying 100 percent weighting to fidelity (i.e. $w_1 = 1$ and $w_2 = 0$) and a robust optimal model is obtained by applying 100 percent weight to robustness (i.e. $w_1 = 0$ and $w_2 = 1$). And, the remaining three combinations result in a compromise between fidelity and robustness objectives. Figure 10 provides a visual comparison of the models produced from these five combinations of weighting functions. Note that this weighted optimization approach originally proposed by Gass and Saaty (1955) offers computational simplicity over multi-objective calibration approach and is known to yield the convex Pareto fronts accurately (Kim and de Weck, 2006).

Figure 11(a) present a comparison of the fidelity and robustness of these five alternative models. It can be observed that the model produced with the fidelity weighting, $w_1 = 0.75$ and the robustness weighting, $w_2 = 0.25$ provides a preferable compromise between fidelity to measurements and robustness to uncertainty in that large gains in the robustness are achieved with only marginal reduction in the performance of the model. The area above the robustness curve continues to decrease as w_2 increases, however, with diminishing returns and with increasingly higher compromise in fidelity. Hence, in this particular application, weighting only 25 percent of the objective function to robustness was sufficient to produce a model with improved robustness while maintaining fidelity to data, as shown in Table III. Figure 11(b)

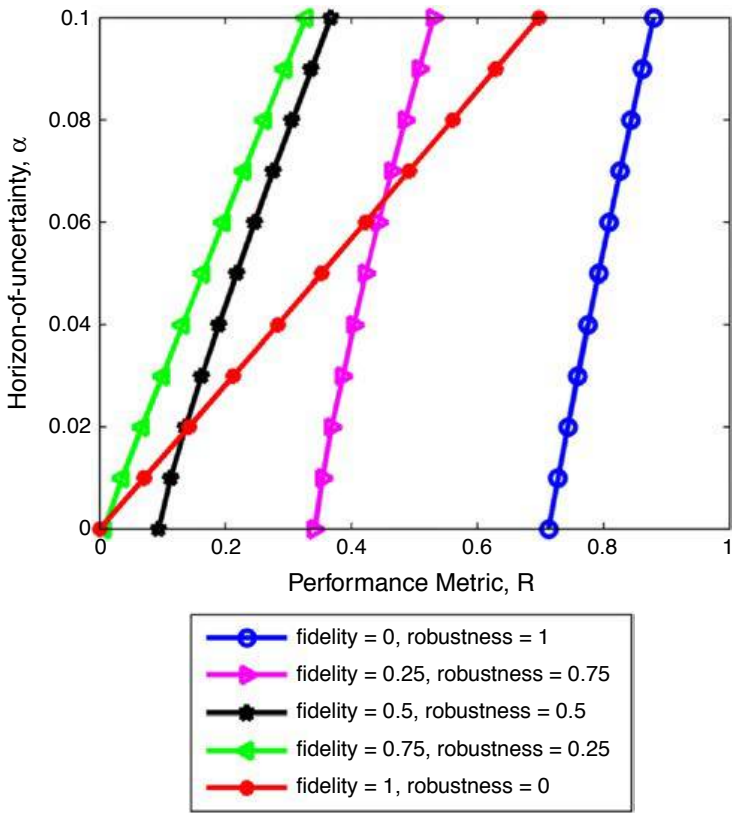

Figure 10.
Info-gap analysis comparing the weighting functions

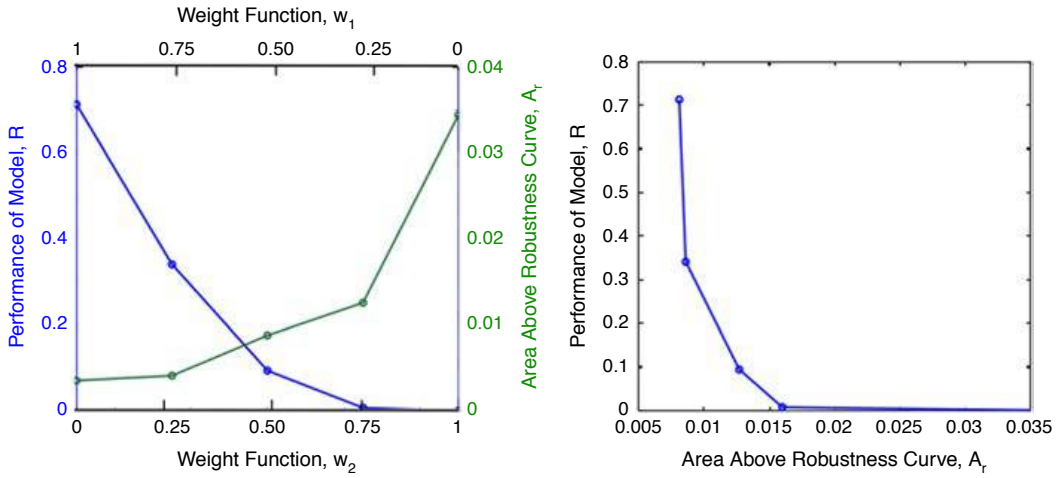

Figure 11.
Comparison of fidelity and robustness

Notes: (a) Applied weighting functions; (b) fidelity and robustness trade-off

demonstrates the relationship between the two competing metrics of the objective function. As the area about the robustness curve increases, the error in model predictions of the model decreases.

5. Geometrically exact 1D beam model

Incorporating geometric nonlinearity is important in modeling wind turbine blades, which routinely experience large deformations and strains. The goal of this section is to test the ability of calibrated parameter values obtained using the 1D linear FE model (discussed in the previous section) to predict response in a nonlinear model by implementing the geometrically exact beam theory (see Fleming and Luscher, 2014, for further details).

In the geometrically exact FE formulation of a beam, sectional strains and curvatures are computed along the position of the beam accounting for local coordinate rotations. Sectional strains are calculated by taking the derivative of the beam's position in space with respect to the undeformed distance along the beam and rotating it to local coordinates. This gives the axial force and transverse shear strains, as seen in Equation (9), where Λ^T is the rotational matrix, r_n' is the position derivative, and b_1 is the direction of the cross-sectional normal:

$$\gamma_n = \Lambda^T r_n{}' - b_1. \tag{9}$$

Sectional curvatures are calculated from the derivative of the rotation tensor with respect to the position along the undeformed beam, giving the torsional rate of twist and bending curvature. The sectional curvatures in local coordinates are shown in Equation (10) where Λ^T is the rotational matrix and Λ_n' is the rotation tensor:

$$\kappa_n = \Lambda^T \Lambda_n{}'. \tag{10}$$

Using the strain energy equation as a basis and differentiating with respect to section strains and curvature, sectional forces and moments are calculated. The local strain energy is related to the cross-sectional properties of the beam at a

given point as well as the section strains and curvature. In Equation (11), the matrix [C] represents a matrix of cross-sectional properties expanded in Equation (12). For isotropic, homogeneous materials, this matrix assumes a diagonal shape:

$$U = \frac{1}{2}\begin{Bmatrix} \gamma \\ \kappa \end{Bmatrix}^T [C] \begin{Bmatrix} \gamma \\ \kappa \end{Bmatrix}, \tag{11}$$

and:

$$\begin{Bmatrix} F_{Na} \\ F_{Nv2} \\ F_{Nv3} \\ F_{Mt} \\ F_{Mb2} \\ F_{Mb3} \end{Bmatrix} = \begin{bmatrix} EA & & & & & \\ & GA_2 & & & 0 & \\ & & GA_3 & & & \\ & & & GJ & & \\ & 0 & & & EI_2 & \\ & & & & & EI_3 \end{bmatrix} \begin{Bmatrix} \gamma_1 \\ \gamma_2 \\ \gamma_3 \\ \kappa_1 \\ \kappa_2 \\ \kappa_3 \end{Bmatrix}. \tag{12}$$

The result of this formulation is a linear force to strain relationship in the moving beam coordinate frame. However, the relationship between generalized strains and generalized coordinates involves the rotation tensor, which is inherently nonlinear.

6. Self-consistency of predictions of the geometrically exact 1D beam model

In Section 4, we obtained five sets of correction factors for the moment of inertia parameters of the 1D linear FE model using five combinations of weighting functions for robustness and fidelity indicators. These five sets of calibrated moment of inertia values are transferred to the geometrically exact beam model to assess the self-consistency of predictions focussing on tip deflection under static loads considering both linear and nonlinear response of the blade. The static deflection is calculated with a load of 20 N to obtain the linear response and 8,000 N to obtain the nonlinear response applied to the free end.

The self-consistency is evaluated by comparing the predictions of the model with increasing levels of uncertainty to the predictions of the model with nominal parameters (recall Equation (3)). The calculated difference is normalized to reflect the percentage change in the predictions. Similar to the analysis provided in Section 4, the info-gap uncertainty model is represented using an envelope-bound uncertainty model, provided in Equation (4).

The results obtained from info-gap analysis for self-consistency are shown in Figure 12 for five models developed with different combinations of weighting factors. Table IV then compares all three attributes; fidelity, robustness, and self-consistency for these five models. Recall that the fidelity and robustness metrics are formulated such that smaller values result in better performance for each category and are obtained with the linear model and calibrated using experimental modal analysis data. In Table IV, the self-consistency results are taken as the area above self-consistency curve, similar to the quantification of robustness, and are obtained with the nonlinear model. Though fidelity and robustness are quantified with the

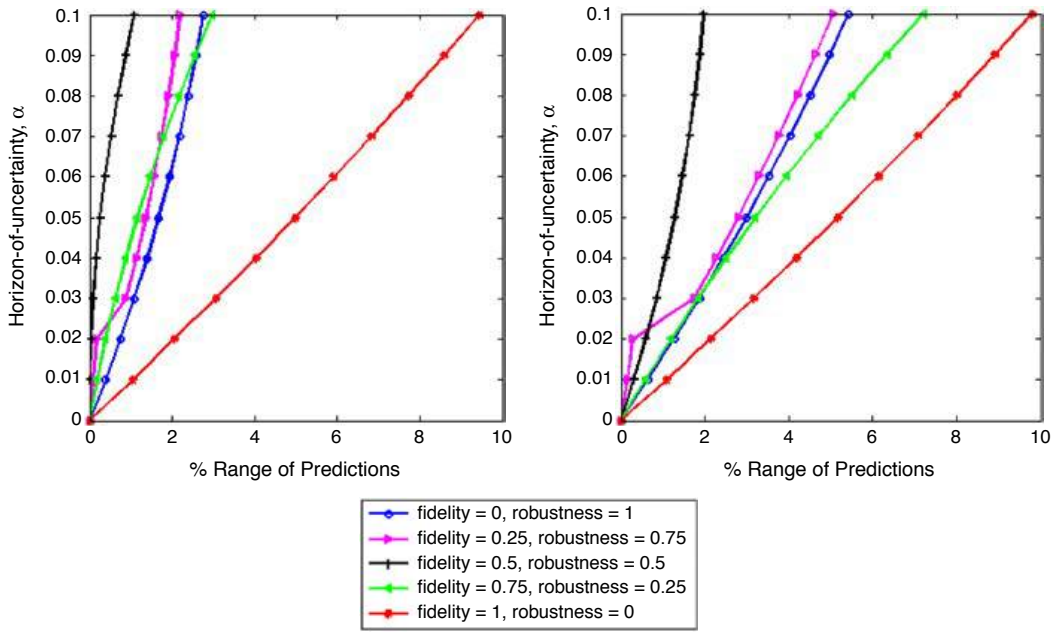

Figure 12.
Self-consistency of predictions in geometrically exact beam model

Case	Weighting functions: Fidelity, w_1	Weighting functions: Robustness, w_2	Fidelity and robustness indicators: Fidelity, R (Hz)	Fidelity and robustness indicators: Robustness, A_r (Hz)	Self-consistency: Linear regime	Self-consistency: Nonlinear regime
1	0	1	0.713	*0.008*	0.520	0.266
2	0.25	0.75	0.341	0.009	0.485	0.212
3	0.5	0.5	0.094	0.013	*0.192*	*0.098*
4	0.75	0.25	0.007	0.016	0.678	0.276
5	1	0	*0.0005*	0.035	0.936	0.902

Table IV.
Comparison of weighting function combinations (best performance indicated in bold)

linear model while self-consistency is quantified with the nonlinear model, the models share common calibrated parameter values in each of the five combinations of weighting factors.

The model produced with $w_1 = 0.5$ and $w_2 = 0.5$ is able to provide the most consistent predictions of tip deflection for both linear and nonlinear regimes. It is important to note that the fidelity optimal model, which provided the lowest robustness to uncertainty, remains the model with the lowest self-consistency of predictions. This result once again suggests that through calibration of model parameters to improve test-analysis correlation, modeling, and simulation community is worsening the self-consistency of the predictions of their models at untested settings. These results stand to warn the readers about model calibration practices which overlook the robustness and self-consistency of predictions for the intended use of the models.

It is also important to note that solely calibrating with respect to robustness did not yield the most self-consistent model. Most importantly, calibrating model parameters considering both fidelity to measurements and robustness of the said fidelity to uncertainty produced the most self-consistent model. Of course,

the ideal compromise between fidelity and robustness objectives during model calibration is dependent on the specifics of the application and must be evaluated as necessary.

7. MCDM

For practical applications of model calibration, decision makers may be faced with the task of selecting the optimal compromise between the two conflicting objectives, fidelity to measurements and robustness of the said fidelity to uncertainty. MCDM is an approach used to determine the most suitable solution in applications requiring satisfaction of conflicting objectives (Laory *et al.*, 2012; Pohekar and Ramachandran, 2004). MCDM provides the decision maker with the ability to place a higher preference on decision criteria with the most importance for an application and aids in differentiating solutions in the decision-making process (Ali and Smith, 2010).

Herein, the WSM, one of the most commonly used MCDM approaches (Pohekar and Ramachandran, 2004), is implemented considering four design criteria (fidelity, robustness, self-consistency in linear regime and self-consistency in nonlinear regime), with the goal being to maximize each of these objectives (by means of minimizing their corresponding indicators). Applying WSM, the best solution is selected based on the following equations:

$$A_i = \sum_{j=1}^{n} a_{ij} w_j \quad for \quad i = 1, 2, 3, \ldots m \tag{13}$$

$$A^* = \min A_i \tag{14}$$

where A_i is the WSM score for each alternative, m is the number of alternatives considered, n is the number of decision criterion, a is the value of a criterion, and w is the weight of importance for a criterion[4]. The goal in this application is to minimize each of criterion therefore, A^* represents the best alternative. It is important to note that in Table IV, the robustness and fidelity indicators were demonstrated with varying scales in each metric. While solving Equation (13), the metrics of each criterion are normalized between 0 and 1 (Table V). All metrics are given an equal weight, w_j, of 0.25.

MCDM is applied to the five alternative solutions explored in Section 6 and the resulting WSM scores and rankings are shown in Table V. Considering all four criteria, the best solution is found to be the third case, where calibration was carried out with equal weighting for fidelity and robustness (refer back to Table IV). This finding

	Fidelity and robustness indicators		Self-consistency		WSM	
Case	Fidelity, R (Hz)	Robustness, A_r (Hz)	Linear regime	Nonlinear regime	Score, A_i	Rank
1	1	0	0.441	0.209	0.412	4
2	0.478	0.037	0.394	0.142	0.263	2
3	*0.012*	*0.185*	*0*	*0*	*0.049*	*1*
4	0.009	0.269	0.653	0.221	0.295	3
5	0	1	1	1	0.750	5

Table V. Weighted sum method scores and ranking

is consistent with observations in Section 6 that the best case predictions are those in which both fidelity and robustness are considered. The ranking based on WSM scores also demonstrates that calibrating model parameters solely considering fidelity results in the worst case performance.

8. Conclusions

This paper aims to raise awareness on the risks of calibrating input parameters of a model to solely improve fidelity to measurements. It is demonstrated on a non-trivial example that a fidelity optimal numerical model is only achieved in association with the extreme deterioration of the robustness of the model to uncertainty.

Accordingly, this paper presents an approach for model calibration considering the trade-off between fidelity to experimental data and robustness of this fidelity to uncertainty remaining in calibrated parameter values. The authors demonstrate the approach on the development of a simplified 1D beam model of the CX-100 wind turbine blade. First, a fidelity optimal model is pursued, in which the model parameters are calibrated to best replicate experimental data. Through use of an info-gap analysis, it is demonstrated that while the fidelity of the calibrated model is improved, the robustness of the model when compared to the initial model is significantly sacrificed, a fact which traditional approaches to model calibration routinely neglects.

The objective function defined for model calibration is then modified as a weighted sum of fidelity and robustness criteria. The inclusion of robustness to uncertainty in the objective function allows for our lack of confidence in calibrated input parameters to be considered in model calibration. Five combinations of weighting functions are evaluated to explore the trade-off between fidelity to measurements and robustness of this fidelity to uncertainty. The robustness is incorporated by considering the area above the robustness curve for the candidate solutions explored by the genetic algorithm. The results demonstrate that achieving optimality in either fidelity or robustness comes with an extreme deterioration in the other objective. However, it is shown that a weighing only 25 percent of the objective function toward robustness yields large gains in robustness with minimal sacrifice in fidelity. Next, the five sets of parameter values calibrated using the 1D linear FE model are transferred to a geometrically exact beam model to assess the self-consistency of predictions. Tip deflection of the blade is evaluated under a hypothetical static loading. It is observed that the fidelity optimal model is the least self-consistent model. This suggests once again that models calibrated only considering the fidelity to measurements are the most susceptible to unknown compensations between various forms of uncertainties and errors present in the model development process. Evaluation of results obtained in this study creates a strong case for new calibration techniques that assess fidelity, robustness and self-consistency.

Finally, the WSM for MCDM was applied to rank the possible solutions obtained through calibration using various robustness and fidelity weights. Fidelity, robustness, self-consistency in linear regime, and self-consistency in nonlinear regime were each evaluated as a decision criterion. Calibration with equal weight given to fidelity and robustness was found to produce the best WSM score. Furthermore, the calibrations only considering robustness or fidelity resulted in the worst WSM scores, once again demonstrating that the prevailing engineering paradigm which implements calibration only considering one objective is fundamentally incomplete.

Simplification of the high-fidelity 3D model to the simplified 1D model would introduce model-form error into the problem due to neglected physics. While the effects of this model-form error were left outside the scope of the work herein, studying the robustness of the model to the neglected physics is a point worthy of future work. Additionally, the optimization in this study is solved using a global, weighted approach, which is only suitable in identifying the convex Pareto fonts. Work is underway in investigating the use of multi-objective optimization approach for simultaneously considering fidelity and robustness criteria (Atamturktur *et al.*, 2014). Furthermore, the analysis completed herein focussed on the modal and static response of the CX-100 blade. Future studies should evaluate the dynamic response taking the dissipative characteristics of the blades into account.

Notes

1. Here, configurations may mean different systems responses or the same response obtained at different settings of the domain of applicability.
2. An important step of model validation that involves comparison of the model predictions to an independent data set to confirm the validity of the measurements is omitted from the discussion herein. A thorough discussion on model validation can be found in Van Buren *et al.* (2012).
3. Note that although both R and A_r have the same units, their allowable ranges are different. Therefore, w_1 and w_2 are not the direct indicators of the relative importance placed on these objectives.
4. It is important to note that the weighting function, w_j, applied for the WSM calculation is not related to the weighting function used to study the trade-off between fidelity and robustness in Sections 4 and 6.

References

Ali, N.B.H. and Smith, I.F.C. (2010), "Dynamic behavior and vibration control of a tensegrity structure", *International Journal of Solids and Structures*, Vol. 47 No. 9, pp. 1285-1296.

Ashwill, T.D. (2009), "Materials and innovations for large blade structures: research opportunities in wind energy technology", *50th AIAA Structures, Structural Dynamics, & Materials Conference*, *Palm Springs, CA*, *May 4-7*.

Atamturktur, S., Hemez, F. and Laman, J. (2012), "Uncertainty quantification in model verification and validation as applied to large scale historic masonry monuments", *Engineering Structures*, Vol. 43, pp. 221-234.

Atamturktur, S., Liu Z., Cogan S. and Juang C.H. (2014), "Calibration of imprecise and inaccurate numerical models considering fidelity and robustness: a multi-objective optimization based approach", *Structural and Multi-disciplinary Optimization*, Vol. 51 No. 3, pp. 659-671.

Atamturktur, S., Hemez, F., Williams, B., Tome, C. and Unal, C. (2011), "A forecasting metric for predictive modeling", *Computers and Structures*, Vol. 89 Nos 23-24, pp. 2377-2387.

Bechly, M.E. and Clausen, P.D. (1997), "Structural design of a composite wind turbine blade using finite element analysis", *Computers & Structures*, Vol. 63 No. 3, pp. 639-646.

Ben-Haim, Y. (2006), *Info-Gap Decision Theory: Decisions Under Severe Uncertainty*, 2nd ed., Academic Press, Oxford.

Ben-Haim, Y. and Hemez, F.M. (2012), "Robustness, fidelity and prediction-looseness of models", *Proceedings of the Royal Society: A Mathematical, Physical and Engineering Science, 2012*, Vol. 468 No. 2137, pp. 227-244.

Brazilevs, Y., Hsu, M.C., Akkerman, I., Wright, S., Takizawa, K., Henicke, B., Spielman, T. and Tezduyar, T.E. (2011), "3D simulation of wind turbine rotors at full scale. Part I: geometry modeling and aerodynamics", *International Journal for Numerical Methods in Fluids*, Vol. 65 Nos 1-3, pp. 207-235.

Caramia, M. and Dell´Olmo, P. (2008), *Multi-objective Management in Freight Logistics: Increasing Capacity, Service Level and Safety with Optimization Algorithms*, Springer, London.

Draper, D. (1995), "Assessment and propagation of model uncertainty", *Journal of Royal Statistical Society B*, Vol. 57 No. 1, pp. 45-97.

Farinholt, K.M., Taylor, S.G., Park, G. and Ammerman, C.M. (2012), "Full-scale fatigue tests of CX-100 wind turbine blades: part I, testing", *Proc. SPIE 8343*, Industrial and commercial applications of smart structures technologies, March 11.

Fleming, I. and Luscher, D.J. (2014), "A model for the structural dynamic response of the CX-100 wind turbine blade", *Wind Energy*, Vol. 17 No. 6, pp. 877-900.

Gass, S. and Saaty, T. (1955), "The computational algorithm for the parametric objective function", *Naval Research Logistics Quarterly*, Vol. 2 Nos 1-2, pp. 39-45.

Goel, T. and Stander, N. (2007), "Multi-objective optimization using LS-OPT", Livermore Software Technology Corporation, Livermore, CA.

Goulet, J.A. and Smith, I.F. (2013), "Structural identification with systematic errors and unknown uncertainty dependencies", *Computers and Structures*, Vol. 128, pp. 251-258.

Griffith, T.D., Carne, T.G. and Paquette, J.A. (2008), "Modal testing for validation of blade models", *Wind Engineering*, Vol. 32 No. 2, pp. 91-102.

Hegenderfer, J. and Atamturktur, S. (2013), "Prioritization of code development efforts in partitioned analysis", *Computer Aided Civil and Infrastructure Engineering*, Vol. 28 No. 4, pp. 289-306.

Hemez, F.M. and Ben-Haim, Y. (2004), "Info-gap robustness for the correlation of tests and simulations of a non-linear transient", *Mechanical Systems and Signal Processing*, Vol. 18 No. 6, pp. 1443-1467.

Higdon, D., Gattiker, J., Williams, B. and Rightley, M. (2008), "Computer model calibration using high dimensional output", *Journal of the American Statistical Association*, Vol. 103, No. 482, pp. 570-583.

Kennedy, M.C. and O'Hagan, A. (2001), "Bayesian calibration of computer models", *Journal of the Royal Statistical Society (Ser. B)*, Vol. 63 No. 3, pp. 425-464.

Kim, I.Y. and de Weck, O.L. (2006), "Adaptive weighted sum method for multiobjective optimization: a new method for Pareto front generation", *Structural Multidisciplinary Optimization*, Vol. 31 No. 2, pp. 105-116.

Laory, I., Ali, N.B.H., Trihn, T.N. and Smith, I.F.C. (2012), "Measurement system configuration for damage identification of continuously monitored structures", *Journal of Bridge Engienering*, Vol. 17 No. 6, pp. 857-866.

Linn, R. and Koo, E. (2011), "WindBlade: coupled turbine/atmosphere modeling", *Paper Presented at the Modeling Turbine-Turbine interactions with Experimental Validation, Los Alamos Annual Workshop, Los Alamos, NM*.

McFarland, J. and Mahadevan, S. (2008), "Multivariate significant testing and model calibration under uncertainty", *Computer Methods in Applied Mechanics and Engineering*, Vol. 197 No. 29, pp. 2467-2479.

Marin, J.C., Barroso, A., Paris, F. and Cañas, J. (2009), "Study of fatigue damage in wind turbine blades", *Engineering Failure Analysis*, Vol. 16 No. 2, pp. 656-668.

Mitchell, M. (1998), *An Introduction to Genetic Algorithms*, 3rd ed., MIT Press, Cambridge, MA.

Mollineaux, M.G., Van Buren, K.L., Hemez, F.M. and Atamturktur, S. (2012), "Simulating the dynamics of wind turbine blades: part II, model development and verification", *Wind Energy*, Vol. 16 No. 5, pp. 694-710.

Pereiro, D., Cogan, S., Sadoulet-Reboul, E. and Martinez, F. (2013), "Robust model calibration with load uncertainties", *Proceedings of the 31st International Modal Analysis Conference, Anaheim, CA, February 11-14*.

Pohekar, S.D. and Ramachandran, M. (2004), "Application of multi-criteria decision making to sustainable energy planning – a review", *Renewable and Sustainable Energy Reviews*, Vol. 8 No. 4, pp. 365-381.

Richardson, T.J., Palmer, M.R., Liepins, G. and Hilliard, M. (1989), "Some guidelines for genetic algorithms with penalty functions", *Proceedings of the Third International Conference on Genetic Algorithms*, Fairfax, VA, June 4-7, pp. 191-197.

Sanderse, B., Pijk, S.P. and Koren, B. (2011), "Review of computational fluid dynamics for wind turbine wake aerodynamics", *Wind Energy*, Vol. 14 No. 7, pp. 799-819.

Shokrieh, M.M. and Rafiee, R. (2006), "Simulation of fatigue failure in a full composite wind turbine blade", *Composite Structure*, Vol. 74 No. 3, pp. 332-342.

Sprague, M.A., Moriarty, P.J., Churchfield, M.J., Gruchalla, K., Lee, S., Lundquist, J.K., Michalakes, J. and Purkayastha, A. (2011), "Computational modeling of wind-plant aerodynamics", *Scientific Discovery through Advanced Computing Program 2011 Conference, Denver, CO, July 10-14*.

US Department of Energy (2008), "20% wind energy by 2030: increasing wind energy's contribution to US electricity supply", Report DOE/GO-102008-2567, US Department of Energy, Washington, DC.

Unal, C., Williams, B., Hemez, F., Atamturktur, S. and McClurea, P.b. (2011), "Improved best estimate plus uncertainty methodology, including advanced validation concepts, to license evolving nuclear reactors", *Nuclear Engineering and Design*, Vol. 241 No. 5, pp. 1813-1833.

Van Buren, K.L. and Atamturktur, S. (2012), "A comparative study: predictive modeling of wind turbine blades", *Wind Engineering*, Vol. 36 No. 3, pp. 235-250.

Van Buren, K.L., Mollineaux, M.G., Hemez, F.M. and Atamturktur, S. (2012), "Simulating the dynamics of wind turbine blades: part II, model validation and uncertainty quantification", *Wind Energy*, Vol. 16 No. 5, pp. 741-758.

Vermeer, L.J., Sorensen, J.N. and Crespo, A. (2003), "Wind turbine wake aerodynamics", *Progress in Aerospace Sciences*, Vol. 39 No. 6, pp. 467-510.

About the authors

Garrison Stevens is a Doctoral Student at the Clemson University in the Glenn Department of Civil Engineering. She is the recipient of GAANN fellowship. She received her BS in Civil Engineering with a structures emphasis from the Clemson University in 2012.

Dr Kendra Van Buren is a Postdoctoral Fellow at the Los Alamos National Laboratory. She received her PhD in Civil Engineering (2012) and MS in Civil Engineering (2009), both with a structures emphasis, from the Clemson University. She received her BS in Civil and Environmental Engineering from the University of California, Los Angeles in 2009.

Elizabeth Wheeler is a Graduate Student at the Clemson University. She received her BS in Civil Engineering with a structures emphasis from the Clemson University in 2014.

Associate Professor Sez Atamturktur is an Associate Professor at the Clemson University and an Advisor of the CU-Ideas research group. Her research group is dedicated to the development, application, and dissemination of model validation and uncertainty quantification (MVUQ) techniques. Dr Atamturktur currently serves as the principal investigator of several federally funded research projects on experiment-based calibration and uncertainty quantification. Dr Atamturktur has published more than 40 peer-reviewed manuscripts and 40 other publications and reports. She currently serves as the Chair of the MVUQ technical division of the Society of Experimental Mechanics. Prior to joining the Clemson University in 2010, she was a LTV Technical Staff Member at the Los Alamos National Laboratory. She received her PhD in Civil Engineering (2009) from The Pennsylvania State University. Associate Professor Sez Atamturktur is the corresponding author and can be contacted at: sez@clemson.edu